AAC Journals.ASM.org

Meropenem and Chromacef Intermediates Observed in IMP-25 Metallo-β-Lactamase-Catalyzed Hydrolysis

Peter Oelschlaeger,[a] Mahesh Aitha,[b] Hao Yang,[b] Joon S. Kang,[c] Antonia L. Zhang,[a] Eleanor M. Liu,[a] John D. Buynak,[d] Michael W. Crowder[b]

Department of Pharmaceutical Sciences, College of Pharmacy, Western University of Health Sciences, Pomona, California, USA[a]; Department of Chemistry and Biochemistry, Miami University, Oxford, Ohio, USA[b]; Department of Biological Sciences, California State Polytechnic University, Pomona, California, USA[c]; Department of Chemistry, Southern Methodist University, Dallas, Texas, USA[d]

Metallo-β-lactamases inactivate most β-lactam antibacterials, and much attention has been paid to their catalytic mechanism. One issue of controversy has been whether β-lactam hydrolysis generally proceeds through an anionic intermediate bound to the active-site Zn(II) ions or not. The formation of an intermediate has not been shown conclusively in imipenemase (IMP) enzymes to date. Here, we provide evidence that intermediates are formed during the hydrolysis of meropenem and chromacef catalyzed by the variant IMP-25 and, to a lesser degree, IMP-1.

Metallo-β-lactamases (MBLs) efficiently inactivate most β-lactam antibacterials and have recently raised concerns due to this broad substrate spectrum, their global spread in various Gram-negative bacteria, and the absence of inhibitors for clinical use (1–3). Zn(II)-bound anionic intermediates of chromogenic β-lactams, such as nitrocefin, have been observed during their hydrolysis catalyzed by the MBLs CcrA (4), L1 (5), NDM-1 (6), and VIM-2 (7). For imipenemase (IMP-1), there might be a nitrocefin intermediate (8), although other studies negate this (9, 10). Tioni and coworkers also observed imipenem and meropenem intermediates in BcII (11). Recently, we found that the variant IMP-25 hydrolyzes meropenem more efficiently than IMP-1 and IMP-6 (12). IMP-6 was previously reported to confer resistance to carbapenems, especially meropenem (13). The increasing k_{cat} for meropenem hydrolysis in the order IMP-1 → IMP-6 → IMP-25 (22 ± 1 s^{-1} → 60 ± 10 s^{-1} → 100 ± 10 s^{-1}, respectively) also translates into increasing MICs of meropenem (16 μg/ml → 64 μg/ml → 128 μg/ml, respectively) (12).

To study in more detail the basis of the increased k_{cat} in IMP-25 versus IMP-1, we carried out pre-steady-state kinetic experiments (6) for the hydrolysis of meropenem [6°C, 25 μM enzyme (E) and substrate (S) ([E]-to-[S] ratio of 1:1) in 50 mM MOPS (morpholinepropanesulfonic acid) (pH 7.0) supplemented with 100 μM Zn(II) ions]. The meropenem substrate (S) was tracked at 310 nm (due to noise at 300 nm), product (P) was tracked at 342 nm, and intermediate (I) was tracked at 390 nm. Details on the determination of extinction coefficients and conversion of the spectral data into concentrations are provided in the supplemental material. With IMP-1, a very small amount of intermediate was observed (Fig. 1E, black line), and the data could not be fitted to a two-phase association/decay function. Substrate disappeared at approximately the same exponential rate (25 ± 3 s^{-1}) at which product appeared (38 ± 12 s^{-1}) (Table 1). In contrast, with IMP-25 (Fig. 1A and B and Table 1), an initial appearance of I at 300 ± 100 s^{-1} was followed by its disappearance at 24 ± 8 s^{-1}. As with IMP-1, the exponential disappearance rate of S (27 ± 1 s^{-1}) was similar to the appearance rate of P (30 ± 20 s^{-1}). Thus, the observed rates of S disappearance and P appearance are indistinguishable between IMP-1 and IMP-25 under these conditions, and the uncertainty of the product formation rates was rather high. However, a clear formation and decay of intermediate was observed in IMP-25. Intermediate accumulated to no more than 6% of the initial [S], which equals [E], meaning that only up to 6% of the E molecules were bound to I.

In order to explore if a clearer picture could be obtained at conditions that are more similar to steady-state conditions, we increased [S] to 100 μM, 200 μM, and 500 μM. Several complications became apparent for the accurate quantification of S and P and, consequently, their disappearance and appearance rates, respectively, at higher concentrations, as detailed in the supplemental material and apparent from the results in Table 1 (results for initial [S] of 500 μM are not shown). The S and I disappearance rates seemed to be similar for the two enzymes, and they agree with steady-state kinetics at the corresponding assay temperature of 6°C for IMP-25 but are about an order of magnitude too high for IMP-1 (see discussion below). The P appearance rates are generally overestimated at higher concentrations (see the supplemental material). However, a qualitative comparison between IMP-1 and IMP-25 up to 200 μM suggests that P is formed 2- to 3-fold faster in IMP-25, which is in agreement with a higher k_{cat} of IMP-25.

In contrast to the challenges with quantifying [S] and [P] at higher concentrations, the feature at 390 nm representing I was clear and within the linear absorbance range (never >0.13). Therefore, we focused our attention on the accumulation of intermediate. The imipenem intermediate in BcII showed an absor-

Received 26 September 2014 **Returned for modification** 1 November 2014
Accepted 12 April 2015

Accepted manuscript posted online 27 April 2015

Citation Oelschlaeger P, Aitha M, Yang H, Kang JS, Zhang AL, Liu EM, Buynak JD, Crowder MW. 2015. Meropenem and chromacef intermediates observed in IMP-25 metallo-β-lactamase-catalyzed hydrolysis. Antimicrob Agents Chemother 59:4326–4330. doi:10.1128/AAC.04409-14.

Address correspondence to Peter Oelschlaeger, poelschlaeger@westernu.edu.

Supplemental material for this article may be found at http://dx.doi.org/10.1128/AAC.04409-14.

doi:10.1128/AAC.04409-14

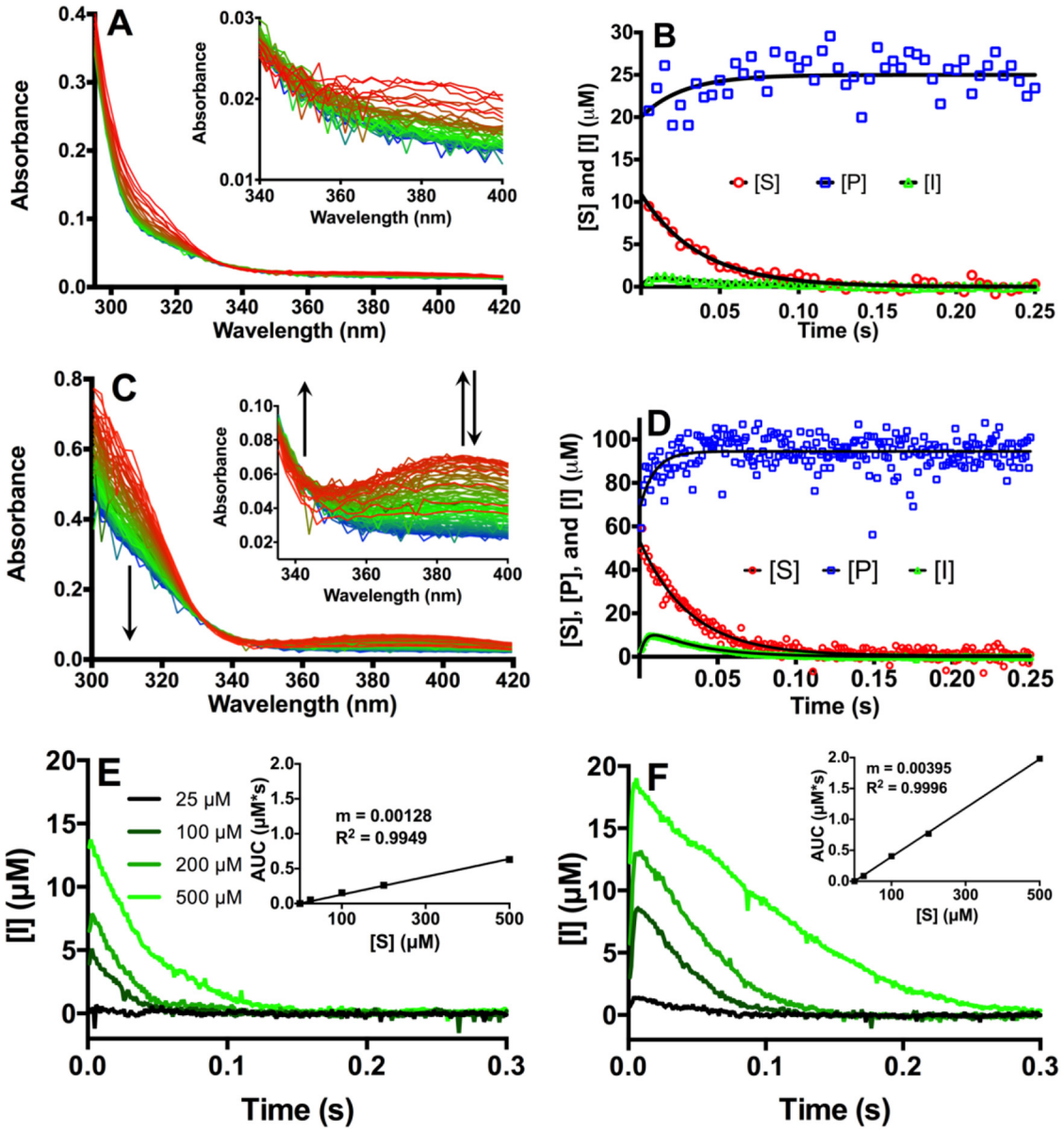

FIG 1 Stopped-flow experiments investigating hydrolysis of meropenem by IMP enzymes. Visible ultraviolet (UV-Vis) spectra were obtained (A and C), and concentrations of substrate ([S]), intermediate ([I]), and product ([P]) were deduced from spectral changes (B and D). (A to D) Hydrolysis of 25 μM (A and B) and 100 μM meropenem (C and D) by 25 μM IMP-25. (A and C) Spectra at different time points are red-green-blue (RGB) color-coded: (A) red, 5 ms; green, 125 ms; blue, 250 ms. (C) red, 1 ms; green, 50 ms; blue, 100 ms. (C) Only the first 100 ms are shown for clarity. The insets show close-ups of the spectra between 340 and 400 nm. The arrows indicate increase or decrease in signals at specific wavelengths. (B and D) Changes in [S], [P], and [I] over time determined from data in panels A and C at 310 nm, 342 nm, and 390 nm, respectively. The black lines are curves fitted with GraphPad Prism version 6.00 for Mac OS X (GraphPad Software, La Jolla, CA, USA) using an exponential decay model for [S], an exponential association model for [P], and a double-exponential association model for [I]. (E and F) Accumulation of intermediate at different substrate concentrations in IMP-1 and IMP-25, respectively. The area under the curve (AUC) values are presented in the insets and exhibit a linear correlation with the initial substrate concentrations ([S]) used.

bance maximum at a similar wavelength (~380 nm) (11), further indicating that the meropenem species at 390 nm is indeed an intermediate. At an initial [S] of 100 μM, a clear appearance and disappearance of I were observed with IMP-25, while S and P were also traced relatively well (Fig. 1C and D). Intermediate accumulated to 8.6% of the initial [S], corresponding to about one-third of E molecules being bound to I. With increasing initial [S], [I] consistently increased for both enzymes, reaching 14 μM at initial [S] of 500 μM (2.8% of initial [S] and 56% of [E], respectively) for IMP-1 (Fig. 1E) and 19 μM (3.8% of initial [S] and 76% of [E]) for IMP-25 (Fig. 1F). The high degree of E saturation suggests that the extinction coefficient chosen for I is a good approximation. Also, the fact that E gets saturated but does not appear to bind more than one I molecule explains why the maximum [I] does not correlate with initial [S] in a linear fashion. However, it is possible that multiple I molecules bound to the same E molecule sequentially over the course of the experiment. Given that k_{cat} is 37 s^{-1} for IMP-25, one catalytic cycle should take 27 ms, and up to 11 inter-

TABLE 1 Summary of pre-steady-state and steady-state kinetic data for meropenem

Enzyme	Pre-steady-state kinetics (6°C)[a]					Steady-state kinetics[b]			
	[S] (μM)	$k_{S,dis}$ (s^{-1})	$k_{I,app}$ (s^{-1})	$k_{I,dis}$ (s^{-1})	$k_{P,app}$ (s^{-1})	Assay temp (°C)	k_{cat} (s^{-1})	K_m (μM^{-1})	k_{cat}/K_m (μM^{-1} s^{-1})
IMP-1	25[c]	25 ± 3	—[d]	—	38 ± 12	30	27.3 ± 0.4	3.2 ± 0.2	8.5 ± 0.5
	100[e]	41 ± 1	—	44 ± 1	*100 ± 20*[f]	6	4.1 ± 0.1	1.8 ± 0.2	2.3 ± 0.3
	200[e]	37 ± 1	530 ± 90	41 ± 1	*71 ± 6*[f]	*6* (calc.)[g]	*2.7*	*1.1*	*2.5*
IMP-25	25[c]	27 ± 1	300 ± 100	24 ± 8	30 ± 20	30	240 ± 20	12 ± 2	21 ± 2
	100[e]	30 ± 1	224 ± 9	30.4 ± 0.4	*340 ± 80*[f]	6	37 ± 2	7 ± 1	5.1 ± 0.4
	200[e]	22 ± 1	158 ± 8	22.9 ± 0.3	*140 ± 20*[f]	*6* (calc.)[g]	*28*	*4.5*	*6.2*

[a] dis and app in subscript indicate disappearance and appearance, respectively, of S, I, and P.
[b] Steady-state kinetics were carried out in triplicate, as detailed in the supplemental material, and the indicated errors are standard deviations.
[c] Experiments were carried out twice, and the indicated errors are deviations between the two experiments.
[d] —, the data could not be fitted.
[e] Experiments were carried out once, and the indicated errors are standard errors of the fits calculated with Prism 6.
[f] Numbers in italics are overestimated due to inconsistent extinction coefficient at high concentrations.
[g] calc., calculated. Details on these calculations are provided in the supplemental material.

mediate molecules could be bound to one E molecule within the 300-ms peak with initial [S] of 500 μM (Fig. 1F). In IMP-1, with a k_{cat} of 4.1 s^{-1} and 244 ms per catalytic cycle, it seems impossible for an E molecule to bind more than one I molecule within the corresponding 150-ms-long peak. When integrating the peaks by determining the area under the curve (AUC), a nearly perfect linear correlation with initial [S] is observed, and the slope is 3.1-fold greater for IMP-25 (Fig. 1E and F, insets). Similar to the disappearance rate of S, the intermediate appearance and disappearance rates do not correlate with the steady-state kinetic rates (Table 1). Thus, the integrated [I] over time and the qualitative P formation rates (at higher concentrations only) seem to be the only reliable indicators for the increased k_{cat} of IMP-25.

In IMP-25, the meropenem I accumulated to a much lower degree (about 6% of the initial [S]) than nitrocefin (~80%) or chromacef (~55%) in NDM-1 (6) with an [E]-to-[S] ratio of 1:1 (Fig. 1B). Intermediate will accumulate if its decay is rate limiting, i.e., if k_3 is $<k_2$ (Fig. 2). In IMP-1, no intermediate is seen with an [E]-to-[S] ratio of 1:1 for meropenem (Fig. 1E) or nitrocefin (9, 10), suggesting that k_3 is $>k_2$. However, the fact that intermediate can accumulate at a higher initial [S] (Fig. 1E) suggests that there is a barrier for intermediate decay of a height very similar to that for intermediate formation, i.e., k_3 can only be slightly bigger than k_2. In IMP-25, this barrier also exists; however, the barrier for intermediate formation has to be equal to or lower than the barrier for intermediate decay, that is, k_2 is $\geq k_3$, in order to allow for relatively more intermediate to form. k_{cat} is related to the rate-limiting microscopic rate constant. In IMP-1, this is k_2; in IMP-25, this is k_3, which is bigger than k_2 in IMP-1. This can explain the bigger k_{cat} in IMP-25 than in IMP-1. It is unclear why this does not result in a higher S disappearance rate in IMP-25 versus IMP-1 in the stopped-flow experiments. Perhaps there is an initial burst

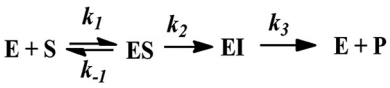

FIG 2 General reaction scheme for the hydrolysis of a substrate by an enzyme with formation of an enzyme-intermediate (EI) complex. Whether EI accumulates depends on the relationship between k_2 and k_3, as explained in the text.

phase, in which a large amount of substrate binds to and is converted by IMP-1 at 25 μM that is not captured in steady-state experiments, in which [E] was 40 nM (almost three orders of magnitude lower). This might play a bigger role in IMP-1 than in IMP-25, which is supported by its 4-fold lower K_m (Table 1). The higher K_m of IMP-25 can in turn also be explained by an increased k_2, as $K_m = (k_2 + k_{-1})/k_1$. Using numbers from IMP-1 and nitrocefin from Griffin et al. (9) for illustration, k_2 would have to increase 450-fold in order to obtain a 4-fold-higher K_m, assuming that the other rates would not be affected. This is consistent with the idea that k_2 would be fast enough to no longer be rate determining.

To further support our hypothesis that the meropenem species observed at 390 nm is indeed a Zn(II)-bound anionic intermediate, we also analyzed the hydrolysis of chromacef (14) (kindly provided by Larry Sutton of Sopharmia, Inc.), which is known to form an anionic intermediate with an absorbance at 575 nm in certain MBLs (6). Besides intermediate, the disappearance of S at 378 nm and appearance of P at 442 nm were monitored using previously published molar extinction coefficients (6). With IMP-1, only a very small increase of absorbance at 575 nm but no subsequent decrease was detected, and there was no crossing of lines at different time points in the spectrum between 442 nm and 575 nm, prompting us to conclude that this signal was attributable to P rather than I (data not shown). The rate constants for S disappearance and P formation were comparable to each other (122 ± 1 s^{-1} and 90 ± 1 s^{-1}, respectively; see Table S1 in the supplemental material) and to k_{cat} at 6°C (131 ± 3 s^{-1}). In contrast, with IMP-25 (Fig. 3), intermediate formed at a very high rate (1,100 ± 100 s^{-1}) and disappeared at a much lower rate (18 ± 7 s^{-1}). The disappearance of S was best fitted to a two-phase decay (>10,000 s^{-1} and 370 ± 10 s^{-1}) and the appearance of P to a two-phase association model (184 ± 4 s^{-1} and 32 ± 20 s^{-1}). Again, intermediate accumulated to only about 5%. The disappearance rate of I is similar to the low product appearance rate but much smaller than the high product appearance rate, which is more similar to the low S disappearance rate and k_{cat} at 6°C. Thus, intermediate is detected, but it appears that the formation of I with an [E]-to-[S] ratio of 1:1 has little impact on the overall enzyme activity.

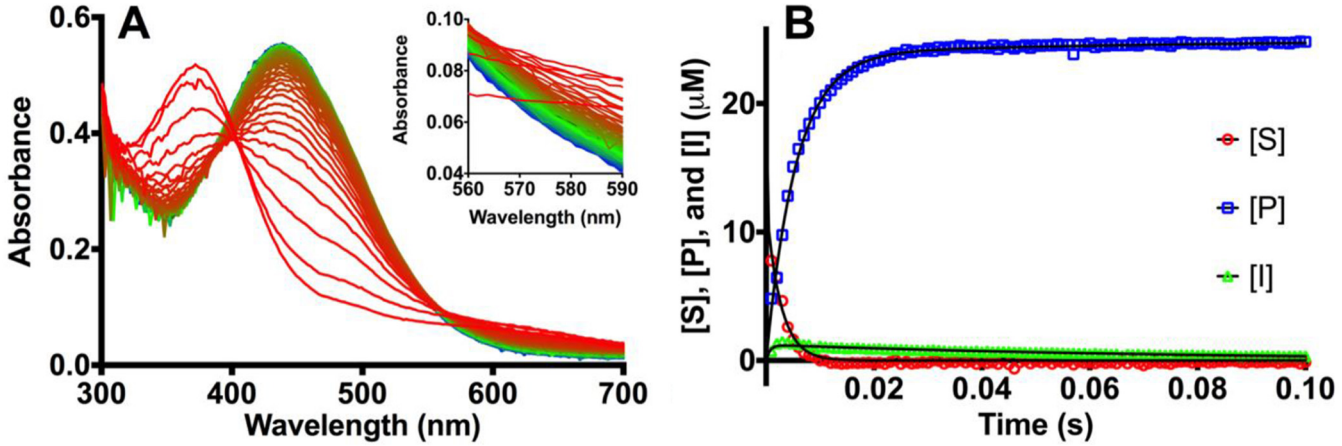

FIG 3 Stopped-flow experiments investigating hydrolysis of chromacef by IMP-25. (A) UV-Vis spectra of hydrolysis of 25 μM chromacef by 25 μM IMP-25. RGB color code: red, 1 ms; green, 50 ms; blue, 100 ms. The inset clarifies the increase, followed by decrease at 575 nm. (B) Changes in [S], [P], and [I] deduced from the spectral changes at 378, 442, and 575 nm, respectively. All data series were fitted to a two-phase decay/association model.

In summary, our results indicate that relatively simple mutations (in this case, S262G and G235S in IMP-25 relative to IMP-1) can significantly alter the energy barriers and kinetic constants of β-lactam hydrolysis by MBLs. In our study, they seemed to stabilize the transition state corresponding to β-lactam amide bond cleavage, thus increasing k_2. Such subtle changes can have a dramatic impact on MICs, as observed for IMP-25 (12), and the clinical significance of these enzymes, e.g., IMP-6 (15). An earlier study by Fast, Wang, and Benkovic (16) showed that a single mutation, C109R (C121R, according to the standard MBL numbering scheme [17]) in the MBL CcrA has a significant effect on the accumulation of nitrocefin intermediate and alters the rate-limiting step from the protonation to formation of I by β-lactam amide bond cleavage, which also results in altered k_{cat} and K_m under steady-state conditions. Thus, mutations of second-shell residues, such as 70, 121, 235, and 262, as they occur in the course of MBL evolution (18, 19) certainly have a role in fine-tuning both the overall activity and catalytic pathway of these enzymes. As new β-lactams and MBL inhibitors, including mechanism-based inhibitors, are being developed, such subtle changes in the catalytic mechanism deserve our attention. On a more fundamental note, our results suggest that all MBLs might employ a catalytic pathway that proceeds through an anionic intermediate; whether I accumulates to levels that are sufficient for detection may depend only on the energy barriers corresponding to I formation and decay.

ACKNOWLEDGMENTS

This work was supported by the National Science Foundation (grant CHE-1151658 to M.W.C.) and the National Institutes of Health (grant R15 AI109624-01A1 to J.D.B.).

We thank Rakesh Mogul and the Department of Chemistry and Biochemistry at California State Polytechnic University, Pomona, CA, for assistance with low-temperature steady-state kinetics and Larry D. Sutton for the gift of chromacef.

REFERENCES

1. **Walsh TR, Toleman MA, Poirel L, Nordmann P.** 2005. Metallo-β-lactamases: the quiet before the storm? Clin Microbiol Rev **18:**306–325. http://dx.doi.org/10.1128/CMR.18.2.306-325.2005.
2. **Oelschlaeger P, Ai N, DuPrez KT, Welsh WJ, Toney JH.** 2010. Evolving carbapenemases: can medicinal chemists advance one step ahead of the coming storm? J Med Chem **53:**3013–3027. http://dx.doi.org/10.1021/jm9012938.
3. **Cornaglia G, Giamarellou H, Rossolini GM.** 2011. Metallo-β-lactamases: a last frontier for β-lactams? Lancet Infect Dis **11:**381–393. http://dx.doi.org/10.1016/S1473-3099(11)70056-1.
4. **Wang Z, Benkovic SJ.** 1998. Purification, characterization, and kinetic studies of a soluble *Bacteroides fragilis* metallo-β-lactamase that provides multiple antibiotic resistance. J Biol Chem **273:**22402–22408. http://dx.doi.org/10.1074/jbc.273.35.22402.
5. **McManus-Munoz S, Crowder MW.** 1999. Kinetic mechanism of metallo-β-lactamase L1 from *Stenotrophomonas maltophilia*. Biochemistry **38:**1547–1553. http://dx.doi.org/10.1021/bi9826512.
6. **Yang H, Aitha M, Hetrick AM, Richmond TK, Tierney DL, Crowder MW.** 2012. Mechanistic and spectroscopic studies of metallo-β-lactamase NDM-1. Biochemistry **51:**3839–3847. http://dx.doi.org/10.1021/bi300056y.
7. **Aitha M, Marts AR, Bergstrom A, Moller AJ, Moritz L, Turner L, Nix JC, Bonomo RA, Page RC, Tierney DL, Crowder MW.** 2014. Biochemical, mechanistic, and spectroscopic characterization of metallo-β-lactamase VIM-2. Biochemistry **53:**7321–7331. http://dx.doi.org/10.1021/bi500916y.
8. **Moali C, Anne C, Lamotte-Brasseur J, Groslambert S, Devreese B, Van Beeumen J, Galleni M, Frere JM.** 2003. Analysis of the importance of the metallo-β-lactamase active site loop in substrate binding and catalysis. Chem Biol **10:**319–329. http://dx.doi.org/10.1016/S1074-5521(03)00070-X.
9. **Griffin DH, Richmond TK, Sanchez C, Moller AJ, Breece RM, Tierney DL, Bennett B, Crowder MW.** 2011. Structural and kinetic studies on metallo-β-lactamase IMP-1. Biochemistry **50:**9125–9134. http://dx.doi.org/10.1021/bi200839h.
10. **Yamaguchi Y, Kuroki T, Yasuzawa H, Higashi T, Jin W, Kawanami A, Yamagata Y, Arakawa Y, Goto M, Kurosaki H.** 2005. Probing the role of Asp-120(81) of metallo-β-lactamase (IMP-1) by site-directed mutagenesis, kinetic studies, and X-ray crystallography. J Biol Chem **280:**20824–20832. http://dx.doi.org/10.1074/jbc.M414314200.
11. **Tioni MF, Llarrull LI, Poeylaut AA, Marti MA, Saggu M, Periyannan GR, Mata EG, Bennett B, Murgida DH, Vila AJ.** 2008. Trapping and characterization of a reaction intermediate in carbapenem hydrolysis by *B. cereus* metallo-β-lactamase. J Am Chem Soc **130:**15852–15863. http://dx.doi.org/10.1021/ja801169j.
12. **Liu EM, Pegg KM, Oelschlaeger P.** 2012. The sequence-activity relationship between metallo-β-lactamases IMP-1, IMP-6, and IMP-25 suggests an evolutionary adaptation to meropenem exposure. Antimicrob Agents Chemother **56:**6403–6406. http://dx.doi.org/10.1128/AAC.01440-12.
13. **Yano H, Kuga A, Okamoto R, Kitasato H, Kobayashi T, Inoue M.** 2001. Plasmid-encoded metallo-β-lactamase (IMP-6) conferring resistance to carbapenems, especially meropenem. Antimicrob Agents

Chemother **45:**1343–1348. http://dx.doi.org/10.1128/AAC.45.5.1343-1348.2001.

14. **Yu S, Vosbeek A, Corbella K, Severson J, Schesser J, Sutton LD.** 2012. A chromogenic cephalosporin for β-lactamase inhibitor screening assays. Anal Biochem **428:**96–98. http://dx.doi.org/10.1016/j.ab.2012.06.006.
15. **Yano H, Ogawa M, Endo S, Kakuta R, Kanamori H, Inomata S, Ishibashi N, Aoyagi T, Hatta M, Gu Y, Yamada M, Tokuda K, Kunishima H, Kitagawa M, Hirakata Y, Kaku M.** 2012. High frequency of IMP-6 among clinical isolates of metallo-β-lactamase-producing *Escherichia coli* in Japan. Antimicrob Agents Chemother **56:**4554–4555. http://dx.doi.org/10.1128/AAC.00617-12.
16. **Fast W, Wang Z, Benkovic SJ.** 2001. Familial mutations and zinc stoichiometry determine the rate-limiting step of nitrocefin hydrolysis by metallo-β-lactamase from *Bacteroides fragilis*. Biochemistry **40:**1640–1650. http://dx.doi.org/10.1021/bi001860v.
17. **Garau G, Garcia-Saez I, Bebrone C, Anne C, Mercuri P, Galleni M, Frere JM, Dideberg O.** 2004. Update of the standard numbering scheme for class B β-lactamases. Antimicrob Agents Chemother **48:**2347–2349. http://dx.doi.org/10.1128/AAC.48.7.2347-2349.2004.
18. **Tomatis PE, Rasia RM, Segovia L, Vila AJ.** 2005. Mimicking natural evolution in metallo-β-lactamases through second-shell ligand mutations. Proc Natl Acad Sci U S A **102:**13761–13766. http://dx.doi.org/10.1073/pnas.0503495102.
19. **Meini MR, Llarrull LI, Vila AJ.** 2014. Evolution of metallo-β-lactamases: trends revealed by natural diversity and *in vitro* evolution. Antibiotics **3:**285–316. http://dx.doi.org/10.3390/antibiotics3030285.